Preparation, Purification, and Characterization of Binuclear Ruthenium(II) Complexes: Bridging Ligands Based on Diazafluorenes

Youxiang Wang, Willie J. Perez, Greg Y. Zheng, D. Paul Rillema,* and Connie L. Huber

Department of Chemistry, Wichita State University, Wichita, Kansas 67260-0051

Received May 8, 1997

A series of bimetallic complexes of ruthenium(II) bridged by heterocyclic ligands formed by the condensation of 4,5-diazafluoren-9-one with various diamines, hydrazine, 1,4-phenylenediamine, benzidine, and 4,4′-methylenedianiline, results in metal centers separated by various distances. The complexes give rise to metal-to-ligand charge-transfer absorptions in the 450 nm region of the visible spectrum and intraligand $\pi \rightarrow \pi^*$ transitions in the 300 nm region of the ultraviolet spectrum. The ruthenium(II) centers are oxidized in two closely spaced one-electron processes at potentials more positive than that for $Ru(bpy)_3^{2+}$. The bridging ligands are reduced by two closely spaced one-electron processes at more positive potentials than that for reduction of the coordinated bipyridine ligands (∼−1.30 V), although the diazafluorene═N−N═diazafluorene bridging ligand is reduced reversibly in two single-electron steps at $E_{1/2}$ values of −0.29 and −0.52 V. After purification by eluting the "pure" complexes over a silica gel column with various concentrations of 0.10 M NH_4PF_6 in methanol, emission occurs only in a glassy matrix at 77 K and at low temperatures in solution. The emission lifetimes at 77 K in a 4:1 ethanol: methanol glass are 5 ± 1 μs. A variable-temperature emission lifetime study reveals the presence of a low-lying state with $\Delta E = \sim 1500$ cm^{-1}, and extrapolation to room temperature indicates the emission lifetimes are in the subnanosecond range.

Introduction

One of the main goals of molecular electronics is the mastery of intramolecular electron transfer over long distances.[1] This requires the assembly of suitable molecular components into an appropriate supramolecular structure.[2] Polypyridyl ruthenium(II) complexes are excellent building blocks for the construction of such devices[3] due to their photochemical properties, and it is, therefore, not surprising that the number of investigations concerning the photochemical and photophysical behavior of binuclear or polynuclear complexes of this type is rapidly growing.[4] Key components of polynuclear complexes are the bridging ligands, since the interactions between the units and, thereby, the properties of the polynuclear complex are critically dependent on the size, shape, and electronic nature of the bridge. Such bridging ligands allow the preparation of polynuclear complexes in which long-range metal−metal interactions in all their forms may be studied, such as optical electron transfer in mixed-valence species,[5] photoinduced electron transfer or energy transfer between an excited-state chromophore and a quencher,[6] and magnetic exchange between paramagnetic centers.[7] The knowledge gained from energy and electron transfer in bimetallic systems has led us to the synthesis of new ligand systems (Scheme 1). Such ligands demonstrate (i) a large variable length allowing connection to metal complexes at variable distances, (ii) conjugated character to explore efficient electron or energy transfer, and (iii) a rigid structure to avoid rotational conformation problems. We had difficulty synthesizing monometallic compounds based on ligands BL_{1-4} because they are poorly soluble in most common solvents, therefore we synthesized monometallic compounds based on ligands L_1 and L_2 for comparison.

Experimental Section

Materials. All reagents and solvents were purchased commercially as HPLC grade and were used without further purification unless otherwise noted. Acetonitrile was dried over 3 Å activated molecular sieves prior to use. Commercially purchased tetrabutylammonium hexafluorophosphate (TBAH) was of electrometric grade (Southwestern Analytical, Inc.) and was used without further purification. Bridging ligands were synthesized as reported.[8] The following compounds were prepared according to literature methods: 4,5-diazafluoren-9-one (dafo),[9] $Ru(bpy)_2Cl_2 \cdot 2H_2O$,[10] and $Ru(bpy)_2CO_3 \cdot 2H_2O$.[11]

Preparation of $[(bpy)_2Ru(BL_1)Ru(bpy)_2](PF_6)_4$. *cis*-Dichlorobis-(2,2′-bipyridine)ruthenium(II) (1.041 g, 2 mmol) and BL_1 (0.360 g, 1

(1) (a) Woitelier, S.; Launay, J.-P. *Inorg. Chem.* **1989**, *28*, 758. (b) Joachim, C.; Launay, J. P.; Woitellier, S. *Chem. Phys.* **1990**, *147*, 131. (c) Ribou, A. C.; Launay, J. P.; Takahashi, K.; Nihira, T.; Tarutani, S.; Spangler, C. W. *Inorg. Chem.* **1994**, *33*, 1325. (d) Collin, J. P.; Laine, P.; Launay, J. P.; Sauvage, J. P.; Sour, A. *J. Chem. Soc., Chem. Commun.* **1993**, 434.

(2) (a) *Supramolecular Photochemistry*; Balzani, V., Ed.; NATO ASI Series; Reidel: Dordrecht, The Netherlands, 1987. (b) Meyer, T. J. *Acc. Chem. Res.* **1989**, *22*, 163. (c) *Supramolecular Photochemistry*; Balzani, V., Scandola, F., Eds.; Horwood: Chichester, U.K., 1990.

(3) (a) Juris, A.; Balzani, V.; Barigelletti, F.; Campagna, S.; Belser, P.; Von Zelewsky, A. *Coord. Chem. Rev.* **1988**, *84*, 85. (b) Ghosh, B. K.; Chakravorty, A. *Coord. Chem. Rev.* **1985**, *95*, 239. (c) DeArmond, M. K.; Carlin, C. M. *Coord. Chem. Rev.* **1981**, *36*, 325.

(4) (a) Bignozzi, C. A.; Paradisi, C.; Roffia, S.; Scandola, F. *Inorg. Chem.* **1988**, *27*, 408. (b) Curtis, J. C.; Bernstein, J. S.; Meyer, T. J. *Inorg. Chem.* **1985,** *24*, 385. (c) Schmehl, R. H.; Auerbach, R. A.; Wacholtz, W. F.; Elliot, C. M.; Freitag, R. A.; Merkert, J. W. *Inorg. Chem.* **1986**, *25*, 2440. (d) Haga, M.; Matsumura-Inoue, T.; Yamabe, S. *Inorg. Chem.* **1987**, *26*, 4148.

(5) (a) Ward, M. D. *Chem. Soc. Rev.* **1995**, 121. (b) Kalyanasundaram, K.; Nazeeruddin, M. K. *Inorg. Chim. Acta* **1994**, *226*, 213.

(6) Sauvage, J. P.; Collin, J. P.; Chambron, J. C.; Guillerez, S.; Coudret, C.; Balzani, V.; Barigelletti, F.; De Cola, L.; Flamigni, L. *Chem. Rev.* **1994**, *94*, 993.

(7) (a) Kahn, O. *Molecular Magnestism*; VCH Publishers: New York, 1993. (b) Das, A.; Maher, J. P.; McCleverty, J. A.; Navas Badiola, J. A.; Ward, M. D. *J. Chem. Soc., Dalton Trans.* **1993**, 681.

(8) Wang, Y.; Rillema, D. P. *Tetrahedron* **1997**, *53*, 12377.

S0020-1669(97)00534-X CCC: $15.00
Published on Web 04/17/1998

Scheme 1

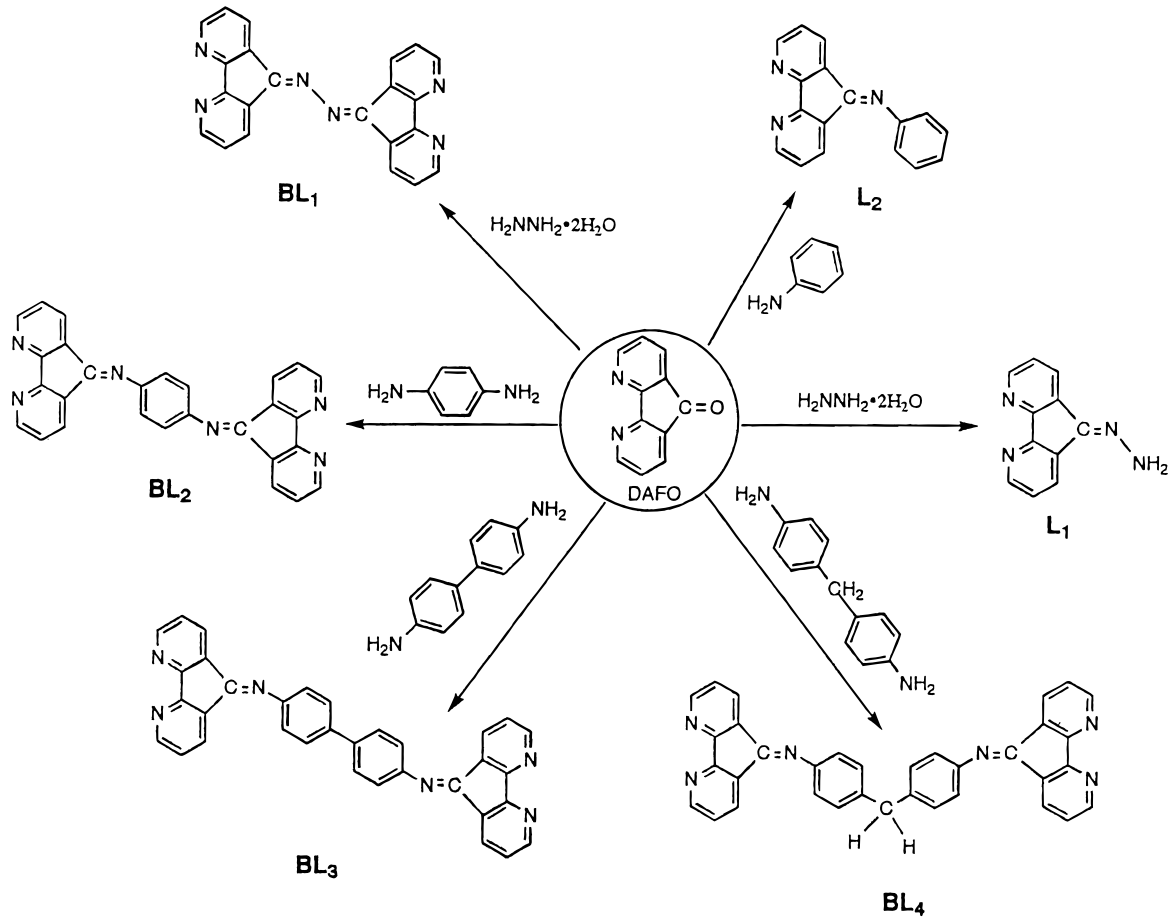

mmol) were refluxed in 30 mL of ethanol for about 5 h. After reflux, the resulting solution was loaded onto a silica gel chromatography column and eluted with ethanol. A purple fraction was collected.[12] Then, the column was eluted with variable concentrations of ammonium hexafluorophosphate in methanol. The proportionally larger orange fraction obtained with 0.1 M NH_4PF_6 was collected, rotary-evaporated to dryness, and redissolved in acetone, and the solution was added dropwise to ethyl ether. The solid which formed was removed by filtration, washed with cold water several times, and dried under vacuum. The overall yield was 0.53 g (30%). Anal. Calcd for $C_{62}H_{44}N_{14}Ru_2P_4F_{24}$: C, 42.14; H, 2.52; N, 11.10. Found: C, 42.07; H, 2.58; N, 11.04.

Preparation of $[(bpy)_2Ru(BL_2)Ru(bpy)_2](PF_6)_4$. *cis*-(Carbonato)-bis(2,2′-bipyridine)ruthenium(II) (114 mg, 0.224 mmol) and BL_2 (50 mg, 0.112 mmol) were refluxed in a solution containing 5 mL of ethanol and 5 mL of nitrobenzene for 1 day under nitrogen gas. The reaction solution was added dropwise to 200 mL of ether. The resulting solution was filtered, the solid was dissolved in a small amount of ethanol, and this solution was loaded onto a silica gel chromatography column and eluted with ethanol. A purple fraction was collected. Then, the column was eluted with variable concentrations of ammonium hexafluorophosphate in methanol. The proportionally larger orange fraction obtained with 0.2 M NH_4PF_6 was collected, rotary-evaporated to dryness, and redissolved in acetone, and the solution was added dropwise to ethyl ether. The solid which formed was removed by filtration, washed with cold water several times, and dried under vacuum. The overall yield was 39 mg (19%). Anal. Calcd for $C_{68}H_{48}N_{14}Ru_2P_4F_{24}$: C, 44.30; H, 2.63; N, 10.64. Found: C, 44.08; H, 2.90; N, 10.39.

Preparation of $[(bpy)_2Ru(BL_3)Ru(bpy)_2](PF_6)_4$. *cis*-(Carbonato)-bis(2,2′-bipyridine)ruthenium(II) (160 mg, 0.306 mmol) and BL_3 (80 mg, 0.153 mmol) were refluxed in a solution containing 5 mL of ethanol and 5 mL of nitrobenzene for 1 day under nitrogen gas. The reaction solution was added dropwise to 200 mL of ether. The resulting solution was filtered, the solid was dissolved in a small amount of ethanol, and this solution was loaded onto a silica gel chromatography column and eluted with ethanol. A purple fraction was collected. Then, the column was eluted with variable concentrations of ammonium hexafluorophosphate in methanol. The proportionally larger orange fraction obtained with 0.1 M NH_4PF_6 was collected, rotary-evaporated to dryness, and redissolved in acetone, and the solution was added dropwise to ethyl ether. The solid which formed was removed by filtration, washed with cold water several times, and dried under vacuum. The overall yield was 70 mg (24%). Anal. Calcd for $C_{74}H_{52}N_{14}Ru_2P_4F_{24}$: C, 46.30; H, 2.74; N, 10.22. Found: C, 45.96; H, 2.66; N, 10.31.

Preparation of $[(bpy)_2Ru(BL_4)Ru(bpy)_2](PF_6)_4$. *cis*-(Carbonato)-bis(2,2′-bipyridine)ruthenium(II) (94 mg, 0.184 mmol) and BL_4 (50 mg, 0.092 mmol) were refluxed in 10 mL of ethanol for about 5 h. The solution was concentrated to half by rotary evaporation. The resulting solution was loaded onto a silica gel chromatography column and eluted with ethanol. A purple fraction was collected. Then, the column was eluted with variable concentrations of ammonium hexafluorophosphate in methanol. The proportionally larger orange fraction obtained with 0.1 M NH_4PF_6 was collected, rotary-evaporated to dryness, and redissolved in acetone, and the solution was added dropwise to ethyl ether. The solid which formed was removed by filtration, washed with cold water several times, and dried under vacuum. The overall yield was 71 mg (40%). Anal. Calcd for

(9) Henderson, L. J.; Fronczek, F. R., Jr.; Cherry, W. R. *J. Am. Chem. Soc.* **1984**, *106*, 5876.
(10) Sullivan, B. P.; Salmon, D. J.; Meyer, T. J. *Inorg. Chem.* **1978**, *17*, 3334.
(11) Kober, E. M.; Caspar, J. V.; Sullivan, B. P.; Meyer, T. J. *Inorg. Chem.* **1988**, *27*, 4587.
(12) The purple eluent was present in each preparation. It was approximately 20% of the products produced and was neutral in charge since it did not precipitate upon addition of NH_4PF_6. Attempts made to determine its identity were unsuccessful.

$C_{75}H_{54}N_{14}Ru_2P_4F_{24}$: C, 46.58; H, 2.82; N, 10.14. Found: C, 46.46; H, 3.00; N, 10.28.

Preparation of $[(bpy)_2Ru(L_1)](PF_6)_2$. *cis*-Dichlorobis(2,2′-bipyridine)ruthenium(II) (0.130 g, 0.25 mmol) and L_1 (0.045 g, 0.25 mmol) were refluxed in 5 mL of ethanol for about 5 h. After refluxing, the resulting solution was loaded onto a silica gel chromatography column and eluted with ethanol. A purple fraction was collected. Then, the column was eluted with variable concentrations of ammonium hexafluorophosphate in methanol. The proportionally larger orange fraction obtained with 0.1 M NH_4PF_6 was collected, rotary-evaporated to dryness, and redissolved in acetone, and the solution was added dropwise to ethyl ether. The solid which formed was removed by filtration, washed with cold water several times, and dried under vacuum. The overall yield was 0.34 g (70%). Anal. Calcd for $C_{31}H_{24}N_8RuP_2F_{12}$: C, 41.38; H, 2.69; N, 12.46. Found: C, 41.27; H, 2.74; N, 12.38.

Preparation of $[(bpy)_2Ru(L_2)](PF_6)_2$. *cis*-Dichlorobis(2,2′-bipyridine)ruthenium(II) (0.130 g, 0.25 mmol) and L_2 (0.077 g, 0.30 mmol) were refluxed in 10 mL of ethanol for about 5 h. After refluxing, the resulting solution was loaded onto a silica gel chromatography column and eluted with ethanol. A purple fraction was collected. Then, the column was eluted with variable concentrations of ammonium hexafluorophosphate in methanol. The proportionally larger orange fraction obtained with 0.1 M NH_4PF_6 was collected, rotary-evaporated to dryness, and redissolved in acetone, and the solution was added dropwise to ethyl ether. The solid which formed was removed by filtration, washed with cold water several times, and dried under vacuum. The overall yield was 0.12 g (52%). Anal. Calcd for $C_{37}H_{17}N_7RuP_2F_{12}$: C, 46.25; H, 2.84; N, 10.21. Found: C, 46.02; H, 2.77; N, 10.12.

Physical Measurements. Visible−UV spectra were obtained with an OLIS modified Cary 14 spectrophotometer. IR spectra were obtained with a Mattson Cynus 25 FT-IR spectrophotometer and were calibrated with the 1601 cm^{-1} band of polystyrene. Differential pulse polarograms were obtained with an EG&G PAR model 263A potentiostat/galvanostat. Coulometry was effected using the above potentiostat and the EG&G PAR Model 377 cell system. The electrochemical measurements were made in a typical H-cell using a platinum disk working electrode, a platinum gauze counter electrode, and a standard saturated sodium calomel electrode (SSCE) and recorded with an IBM 325T computer. The supporting electrolyte was 0.1 M TBAH. All samples were purged with nitrogen prior to measurement. Emission spectra were obtained for each complex in acetonitrile at room temperature and in a 4:1 ethanol:methanol glass at 77 K with a SPEX Fluorolog 212 spectrofluorometer. All emission spectra were corrected for instrument response. Excited-state lifetimes were determined by exciting the samples at 450 nm using an OPOTEK optical parametric oscillator pumped by a frequency-tripled Nd:YAG laser (Continuum Surlite, run at ≤1.5 mJ/10 ns pulse). Spectral regions were isolated using a Hamamatsu R955 PMT in a cooled housing (−15 °C, Amherst) coupled to an Acton SpectraPro 275 monochromator. Transients were recorded with a LeCroy 9359A digital oscilloscope (1 Gs/s). Oscilloscope control and data curve fitting were accomplished with a program developed in-house. All emission samples were prepared in HPLC grade, or better, solvents, filtered through 0.45 μ PTFEE filters, and then freeze−pump−thaw degassed prior to measurement. Errors in measurements are ±1 in the last digit, unless indicated. Variable-temperature emission lifetimes from 90 to 200 K were determined by adding a Cryo Industries EVT cryostat controlled by a Lakeshore 805 temperature controller to the system above. The cryostat was modified in-house by adding a larger copper thermal mass and then calibrated with an auxiliary thermocouple using ice-cold water as the reference junction. This resulted in a temperature accuracy of ±1.6 K over the 90−290 K range. Equation 1 was used to calculate the emission quantum yields,[13] where A is the absorbance at the excitation wavelength, I is the integrated emission intensity, and η is the index of refraction of the solvent. Emission quantum yields were calculated relative to a rhodamine B standard ($\Phi_{std} = 0.71$)[14] in 4:1 ethanol:methanol.

$$\Phi_{em} = (\eta_{cmpd}^2/\eta_{std}^2)(R_{std}/R_{cmpd})(I_{cmpd}/I_{std})\Phi_{std} \qquad (1)$$

Evaluation of Temperature-Dependent Emission Data. The temperature-dependent emission lifetimes obtained in the mixed solvents of 4:1 ethanol/methanol for each complex were plotted versus the absolute temperatures. The temperature-dependent profiles generated for each complex were fit to eq 2

$$\tau^{-1} = k_o + k_1 e^{-\Delta E/RT} \qquad (2)$$

by using the program ORIGIN. In eq 2, k_o is the sum of radiative and nonradiative rate constants and set equal to the observed emission decay rate constant at 77 K. The parameters k_1 and ΔE, which are related to the thermal deactivation process of the emitting state, were determined from a curve-fitting analysis of the data.

Results

Metal−Metal Distances. Attempts were made to grow single crystals of the complexes, but these were unsuccessful. Therefore, MM2 calculations (MCModel, Version 3.0; Serena Software) were performed for determining the distances between the two ruthenium ions in the dimer complexes. The Ru−N bonds were not externally parametrized in any way, although the oxidation state of ruthenium and its covalent radius (1.355 Å for Ru^{II} per manual) were used in the calculation. To prevent falling into a trap of a local minimum, each structure was placed in a randomizing routine after initial minimization. This was performed iteratively for each atom movement. Once complete, the structure with the minimum energy (via randomization) was displayed. The initial minimizations and the randomizations were done in triplicate, and each time the minimum energies were within approximately 1% of each other. MM2 calculations for the dimer complexes led to the distances between the two ruthenium ions of 12.4 Å for $[(bpy)_2Ru]_2BL_1^{4+}$, 14.9 Å for $[(bpy)_2Ru]_2BL_2^{4+}$, 19.2 Å for $[(bpy)_2Ru]_2BL_3^{4+}$, and 17.7 Å for $[(bpy)_2Ru]_2BL_4^{4+}$. The MM2 calculations indicated the that BL_1 moiety is not planar. The two diazafluorenes were twisted with a dihedral angel of 2.5°. The biphenyl unit in BL_3 had a dihedral angel of 44°. The minimized energies increased in the order $[(bpy)_2Ru]_2BL_1^{4+} < [(bpy)_2Ru]_2BL_2^{4+} < [(bpy)_2Ru]_2BL_3^{4+} < [(bpy)_2Ru]_2BL_4^{4+}$. The increases in energy were in agreement with an increase in the complexity of the systems.

UV−Visible Spectra of Complexes. The absorption spectra are illustrated in Figure 1, and absorption data listing energy maxima and absorption coefficients are summarized in Table 1. The absorption coefficients were obtained from Beer's law studies and determined from at least four dilution points. Two distinct sets of absorption bands were present for all of the ruthenium complexes. The probable assignments[15] for the absorption bands were made on the basis of the well-documented optical transitions in $[Ru(bpy)_3]^{2+}$. The set at higher energy can be attributed to intraligand $\pi \rightarrow \pi^*$ transitions; the set at lower energy can be assigned as metal-to-ligand charge-transfer, $d\pi \rightarrow \pi^*$, transitions. The positions and shapes of the $d\pi \rightarrow \pi^*$ transitions did not differ greatly between the complexes but are all blue-shifted ∼10 nm compared to those of $[Ru(bpy)_3]^{2+}$. This is reasonable since the ligands are similar to 2,2′-bipyridine.

Electrochemistry. Reduction potentials for the complexes in CH_3CN were obtained by cyclic voltammetry and differential

(13) Demas, J. N.; Crosby, G. A. *J. Phys. Chem.* **1971**, *75*, 991.

(14) Calvert, J. G. *Photochemistry*; Wiley: New York, 1966.

(15) (a) Seddon, E. A.; Seddon, K. R. *The Chemistry of Ruthenium*; Elsevier: Amsterdam, 1984. (b) Kober, E. M.; Meyer, T. J. *Inorg. Chem.* **1982**, *21*, 3967.

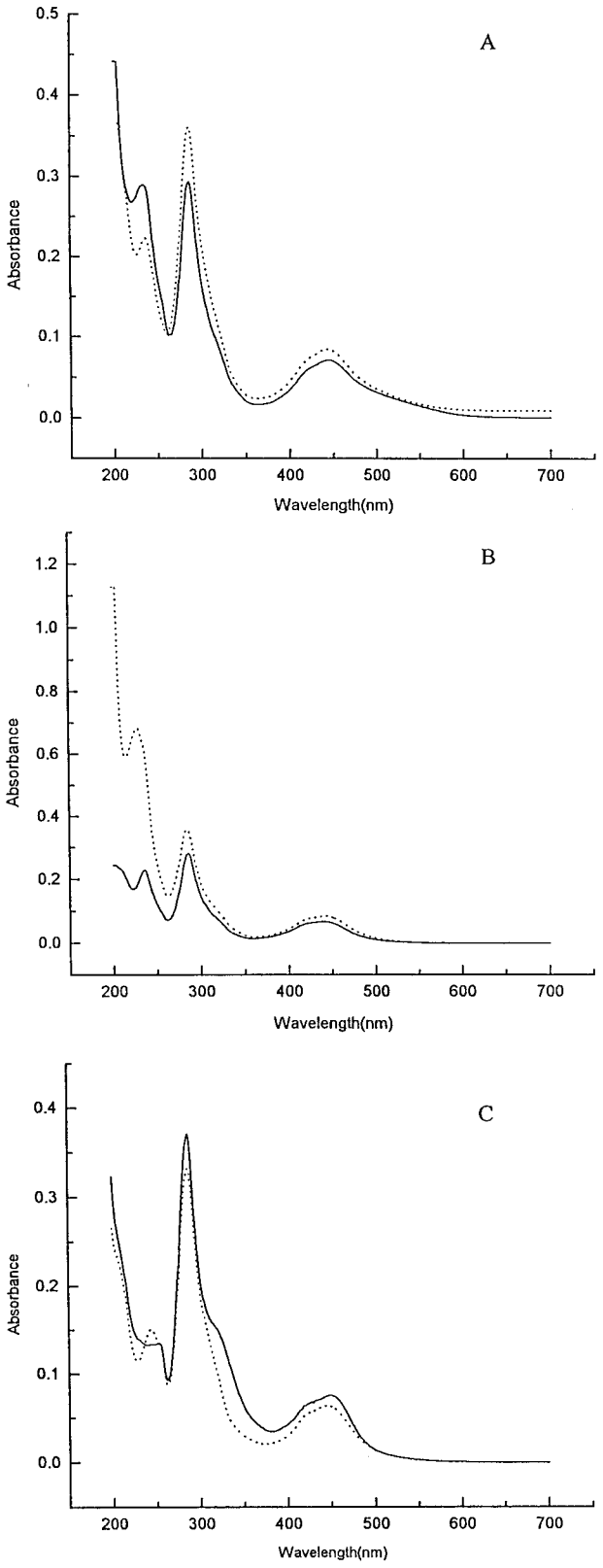

Figure 1. Absorption spectra of the complexes in acetonitrile: (A) $[(bpy)_2Ru]_2BL_2^{4+}$ (solid line, 1.94×10^{-5} M), $[(bpy)_2Ru]_2BL_3^{4+}$ (dotted line, 1.98×10^{-5} M); (B) $[(bpy)_2Ru]_2BL_4^{4+}$ (dotted line, 1.10×10^{-5} M), $[(bpy)_2Ru(L_2)]^{2+}$ (solid line line, 1.90×10^{-5} M); (C) $[(bpy)_2Ru(L_1)]^{2+}$ (solid line, 5.30×10^{-5} M), $[(bpy)_2Ru]_2BL_1^{4+}$ (dotted line, 2.00×10^{-5} M).

pulse polarography. Results are listed in Table 2. Reversibility was assessed on the basis of the oxidation/reduction peak spacings of $59/n$ mV, where n is the number of electrons transferred, and the ratios of i_{red}/i_{ox} which were near 1 for a reversible couple.[16] The number of electrons involved in a redox process was assessed by coulometry in selected cases and then by peak current comparisons. The assignments of ruthenium(III/II) couples and bipyridine ligand reductions were made on the basis of the well-established redox properties of polypyridyl ligand complexes.[17]

Table 1. UV−Visible Spectral Data for Ruthenium Complexes[a]

complex	λ_{max}, nm (ϵ, M^{-1} cm^{-1})		
$[(bpy)_2Ru]_2BL_1^{4+}$	444 (3.5×10^4)	285 (1.4×10^5)	243 (6.7×10^4)
$[(bpy)_2Ru]_2BL_2^{4+}$	442 (3.8×10^4)	285 (1.2×10^5)	239 (8.9×10^4)
$[(bpy)_2Ru]_2BL_3^{4+}$	444 (3.7×10^4)	285 (1.2×10^5)	239 (1.1×10^4)
$[(bpy)_2Ru]_2BL_4^{4+}$	441 (3.6×10^4)	285 (1.4×10^5)	239 (1.1×10^4)
$[(bpy)_2Ru(L_1)]^{2+}$	448 (1.5×10^4)	286 (7.1×10^4)	252 (2.6×10^4)
$[(bpy)_2Ru(L_2)]^{2+}$	441 (2.0×10^4)	286 (7.8×10^4)	235 (2.5×10^4)

[a] In acetonitrile; $T = 298 \pm 1$ K. Errors: λ_{max}, ± 1 nm; ϵ, ± 0.1 M^{-1} cm^{-1}.

The cyclic voltammogram of the complex $[(bpy)_2Ru(BL_1)Ru(bpy)_2](PF_6)_4$ is compared to the one for the BL_1 ligand in Figure 2. An oxidation and four reductions for the complex are observed. For the BL_1 dimer, coulometry carried out at -0.62 V ($n = 1.98$) revealed that the two reductions at -0.29 and -0.52 V were each a one-electron process associated with the BL_1 ligand but were shifted positively compared to those for the uncoordinated ligand due to the presence of the positively charged ruthenium centers. The single oxidation is composed of two closely spaced one-electron processes associated with each of the ruthenium centers. The remaining two waves located at -1.45 and -1.68 V consisted of two closely spaced one-electron processes for each wave related to reduction of the bipyridine ligands on each ruthenium center. The reductions of the bipyridine ligands occurred sequentially at each metal center prior to reduction of the second bipyridine ligand. The cyclic voltammograms for the BL_2 and BL_3 dimers can be interpreted in a similar manner as the one for the BL_1 dimer except the two single-electron waves between the metal oxidations and the bpy reductions were replaced by a two one-electron process. For the BL_4 dimer, an irreversible reduction with a peak at -0.94 V and a return wave at -0.35 V were observed. Similarly the $[Ru(bpy)_2L_1]^{2+}$ and $[Ru(bpy)_2L_2]^{2+}$ monomers also displayed this same irreversible behavior. Compared to those for $[Ru(bpy)_3]^{2+}$, reduction processes and oxidation processes for all the complexes occur at less negative potentials.

Emission Properties at 77 and 298 K. The emission spectra of the complexes at 77 K displayed vibrational components similar to those reported for $[Ru(bpy)_3]^{2+}$, [3a] whereas the complexes at room temperature showed no emission at all. The positions of the first vibrational maximum obtained at 77 K are tabulated in Table 3. An entry is also made for ruthenium tris(bipyridine) for comparison. Figure 3 shows the emission spectra of $[Ru(bpy)_3]^{2+}$ and $[Ru(bpy)_2L_2]^{2+}$ at 77 K in 4:1 EtOH/MeOH. Compared to those for $[Ru(bpy)_3]^{2+}$, emission maxima were all blue-shifted ~10 nm and the positions of the emission energy maxima were relatively constant for all the complexes at 77 K. Emission decays were monoexponential at 77 K, and the emission lifetimes varied from 4 to 6 μs. At room

(16) Christopher, M. A. B.; Ana, M. O. B. *Electrochemistry: Principles, Methods, and Application*; Oxford University Press: New York, 1993.
(17) (a) Balzani, V.; Juris, A.; Venturi, M.; Campagna, S.; Serroni, S. *Chem. Rev.* **1996**, *96*, 759. (b) Balzani, V.; Ballardini, R.; Bolleta, F.; Gandolfi, M. T.; Juris, A.; Maestry, M.; Mamfrin, M. F.; Moggi, L.; Sabbatini, N. *Coord. Chem. Rev.* **1993**, *113*, 227.

Table 2. Redox Potentials for Ruthenium Complexes[a]

	$E_{1/2}$, V (ΔE_p, mV)				
complex	oxidation	Reductions			
$[(bpy)_2Ru]_2BL_1^{4+}$	1.38 (60)	−0.29 (60)	−0.52 (60)	−1.45 (65)	−1.68 (60)
$[(bpy)_2Ru]_2BL_2^{4+}$	1.32 (56)	−0.73 (42)	−1.24 (96)	−1.50 (56)	−1.75 (64)
$[(bpy)_2Ru]_2BL_3^{4+}$	1.37 (58)	−0.67 (52)	−1.27 (100)	−1.53 (134)	−1.68 (68)
$[(bpy)_2Ru]_2BL_4^{4+}$	1.32 (72)	−0.94[b]		−1.56[b]	−1.74 (54)
$[(bpy)_2Ru(L_1)]^{2+}$	1.32 (87)	−0.86[b]		−1.45 (50)	−1.68 (100)
$[(bpy)_2Ru(L_2)]^{2+}$	1.36 (72)	−0.88[b]		−1.46 (90)	−1.70 (100)
$Ru(bpy)_3^{2+}$	1.28 (60)		−1.32 (60)	−1.52 (60)	−1.77 (60)

[a] All samples measured in 0.1 M TBAH/CH_3CN; error in potentials was ±0.02 V; $T = 23 \pm 1$ °C; scan rate = 200 mV/s.

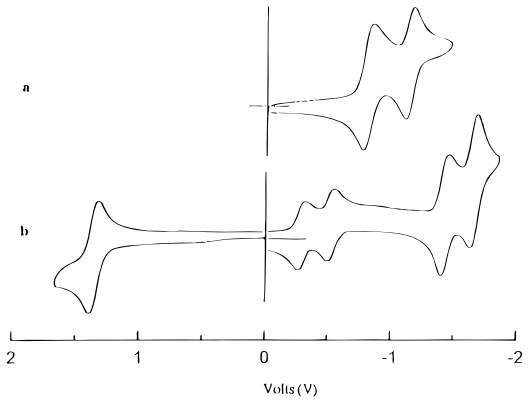

Figure 2. Cyclic voltammograms of BL_1 (a) and $[(bpy)_2Ru]_2BL_1^{4+}$ (b) in acetonitrile at room temperature.

temperature, emission lifetimes for all the complexes were too short to measure.

Temperature-Dependent Emission Lifetimes. Emission maxima were dependent on the temperature as shown for $[(bpy)_2Ru]_2BL_1^{4+}$ in Figure 4. Emission maxima red-shifted as the temperature increased. For $[(bpy)_2Ru]_2BL_1^{4+}$, the emission maximum shifted from 567 nm at 77 K to 649 nm at 200 K, which is consistent with the metal-to-ligand charge-transfer nature of the process where solvent plays a critical role in the response to the photoinduced dipole change.

Emission lifetimes were measured at different temperatures in 4:1 ethanol/methanol over the 90−200 K range and are shown in Figure 5. Starting at 90 K, the emission lifetimes of a specific complex remained nearly the same in the glassy matrix through the glass-to-fluid region (∼130 K). Above 140 K in the fluid region, emission lifetimes decreased rapidly. The temperature-dependent lifetime behavior was fit to eq 2, and the results are given in Table 3. The activation energy for all compounds fell in the range 1490−1650 cm^{-1}, but the preexponential constants varied from 5.7×10^{11} to 3.1×10^{13} s^{-1}.

Discussion

Synthesis and Purification of Complexes. The complexes were prepared by refluxing the starting materials in different solvents due to differences in solubility of the bridging ligands resulting from the degree of conjugation.[18] Nitrobenzene proved to be a good solvent for the extended aromatic systems and was removed by evaporation after the reaction. Several methods were tried in attempts to remove residual monometallic impurities. These included ion-exchange Sephadex CP-25 chromatography,[19] size-exclusion chromatography on Sephadex LH-20 eluted with volume ratios 4:4:1 (acetone:CH_2Cl_2:MeOH),[20] neutral alumina chromatography with eluent as 1:1 (CH_2Cl_2:tolune)[21] volume ratios, and silica gel chromatography with eluent as 5:4:1 (CH_3CN:H_2O:KNO_3)[22] volume ratios. In all cases, the complexes obtained gave excellent elemental analyses and acceptable IR, NMR, and visible−UV results but always contained a luminescing impurity in their emission spectra. A solution to this problem was found by purifying the complexes on a silica gel column after reaction by eluting with various concentrations of NH_4PF_6 in methanol, which resulted in removal of luminescing impurities as shown in Figure 6. The complexes purified in this way show no emission at room temperature. This method *may be extremely useful* since in the past it has always been necessary to take into consideration the possibility of strong luminescence in Ru(II) polypyridyl complexes which could result from several members of the family,[23] in particular $Ru(bpy)_3^{2+}$.

Redox Properties. The cyclic voltammograms of bimetallic complexes in acetonitrile all exhibit a reversible two one-electron oxidation around +1.35 V corresponding to the Ru(II/III) couple. As anticipated, this potential is slightly more positive (by about 70 mV) than that for the corresponding process in $Ru(bpy)_3^{2+}$ due to the higher π acidity of the bridging ligands than of bipyridine. But, compared to that for $Ru(bpy)_2(dafo)^{2+}$, which can be regarded as the parent complex, this potential is slightly more negative (by about 60 mV), which indicates that the bridging ligands are less acidic than dafo. Therefore the ligand π acidities follow the order bpy < BL_{1-4}, L_{1-2} < dafo. In the absence of any metal−metal interaction, one would anticipate that symmetric bimetallic complexes would exhibit metal-based oxidations at the same potential for both metal centers. If there is metal−metal communication through the bridging ligand, such symmetric bimetallic complexes would be expected to exhibit two oxidations since the oxidation of one metal center will be influenced by the oxidation of the other. In the current study, bimetallic complexes exhibited a single, unperturbed wave in cyclic voltammetry and a single peak

(18) Carey, F. A. *Organic Chemistry*, 2nd ed.; McGraw-Hill: New York, 1992.

(19) (a) Didier, P.; Jacquet, L.; Mesmaeker, A. K.-D.; Hueber, R.; Dorsselaer, A. V. *Inorg. Chem.* **1992**, *31*, 4803. (b) Ohno, T.; Nozaki, K.; Haga, M.-A. *Inorg. Chem.* **1992**, *31*, 4256. (c) Didier, P.; Jacquet, L.; Mesmaeker, A. K.-D. *Inorg. Chem.* **1995**, *34*, 3695.

(20) (a) Bardwell, D. A.; Barigelletti, F.; Rosemary, L. C.; Flamigni, L.; Guardigli, M.; Jeffery, J. C.; Ward, M. C. *Inorg. Chem.* **1995**, *34*, 2438. (b) Balzani, V.; Bardwell, D. A.; Barigelletti, F.; Rosemary, L. C.; Guardigli, M.; Jeffery, J. C.; Sovrani, T.; Ward, M. C. *J. Chem. Soc., Dalton Trans.* **1995**, 3601.

(21) Strouse, G. F.; Schoonover, J. R.; Duesing, R.; Boyde, S.; Jones, W. E.; Meyer, T. J. *Inorg. Chem.* **1995**, *34*, 473.

(22) Elliott, C. M.; Ferrere, S. *Inorg. Chem.* **1995**, *34*, 5818−5824 and references therein.

(23) (a) Belser, P.; Zelewsky, A. V.; Juris, A.; Barigelletti, F.; Balzani, V. *Chem. Phys. Lett.* **1984**, *104*, 100. (b) Caspar, J. V.; Meyer, T. J. *J. Am. Chem. Soc.* **1983**, *105*, 5583.

Table 3. Temperature-Dependent Emission Properties[a,b]

complex	k_1, 10^{12} s^{-1}	ΔE, 10^3 cm^{-1}	λ_{max}, (77 K), nm	τ_{77K}, μs[c]	τ_{298K}, ns[c,d]
$[(bpy)_2Ru]_2BL_1^{4+}$	4.30	1.52±0.09	568,611	5.5±0.4	0.36
$[(bpy)_2Ru]_2BL_2^{4+}$	19.00	1.60±0.07	568,614	5.3±0.2	0.12
$[(bpy)_2Ru]_2BL_3^{4+}$	31.00	1.64±0.06	567,610	5.7±0.3	0.10
$[(bpy)_2Ru]_2BL_4^{4+}$	9.00	1.65±0.15	567,610	4.1±0.4	0.33
$[(bpy)_2Ru(L_1)]^{2+}$	0.57	1.49±0.20	567,610	4.9±0.5	2.5
$[(bpy)_2Ru(L_2)]^{2+}$	5.80	1.49±0.04	566,612	4.2±0.5	0.24
$[Ru(bpy)_3]^{2+}$	6.72	3.60±0.04	576	5.1±0.5	890

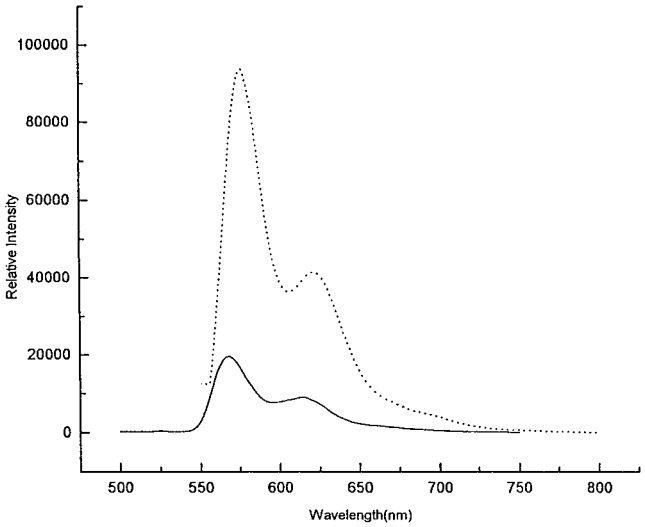

Figure 3. Emission spectra of $[Ru(bpy)_3]^{2+}$ (dotted line) and $[(bpy)_2Ru(L_2)]^{2+}$ (solid line) at 77 K in 4:1 EtOH/MeOH.

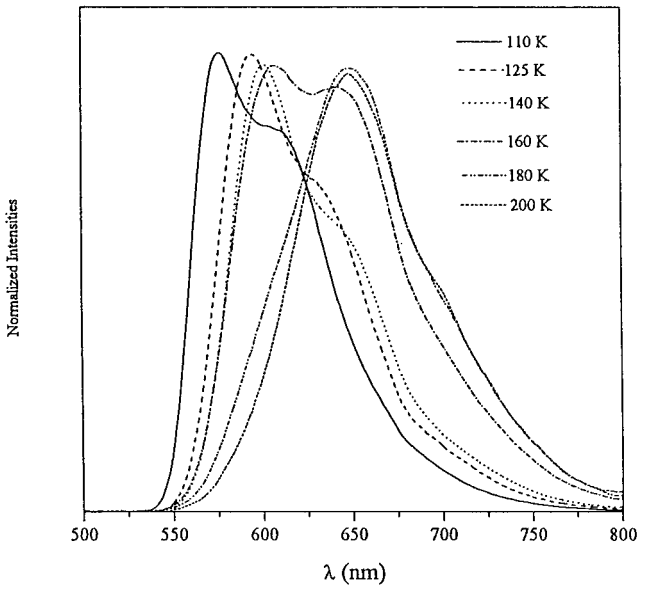

Figure 4. Normalized luminescence spectra of $[(bpy)_2Ru]_2BL_1^{4+}$ as a function of temperature. The solvent is EtOH/MeOH (4:1).

without broadening in differential pulse polarography. On the basis of the above results, the following assignments for oxidations can be made, where b represents the bipyridine ligand and BL the bridging ligand:

$$[(b)(b)Ru^{II}(BL)Ru^{II}(b)(b)]^{4+} - e^- = [(b)(b)Ru^{III}(BL)Ru^{II}(b)(b)]^{5+} \quad (3)$$

$$[(b)(b)Ru^{III}(BL)Ru^{II}(b)(b)]^{5+} - e^- = [(b)(b)Ru^{III}(BL)Ru^{III}(b)(b)]^{6+} \quad (4)$$

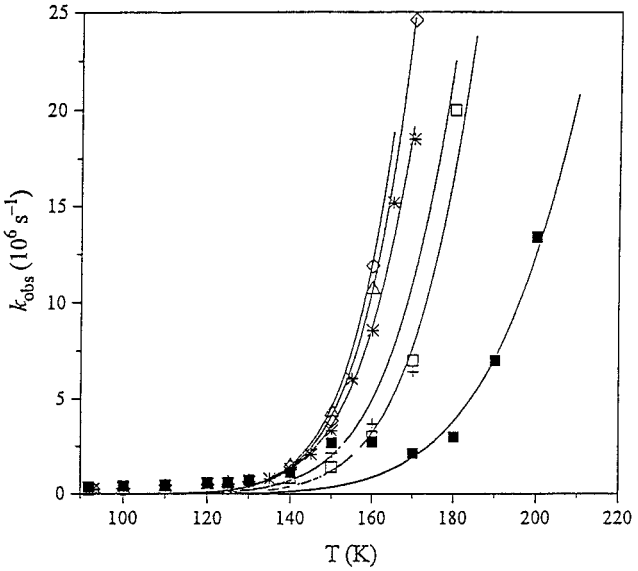

Figure 5. Emission lifetimes of $[(bpy)_2Ru]_2BL_1^{4+}$ (+), $[(bpy)_2Ru]_2BL_2^{4+}$ (◇), $[(bpy)_2Ru]_2BL_3^{4+}$ (△), $[(bpy)_2Ru]_2BL_4^{4+}$ (□), $[(bpy)_2Ru]L_1^{2+}$ (*), and $[(bpy)_2Ru]L_2^{2+}$(■) as a function of temperature. The solvent is EtOH/MeOH (4:1).

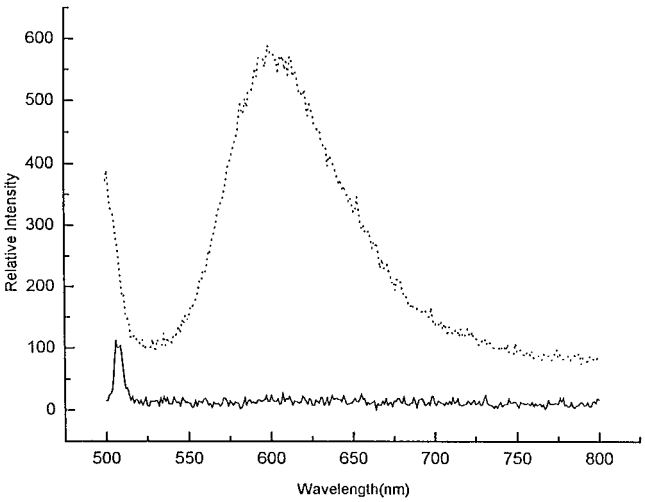

Figure 6. Room-temperature emission spectra of $[(bpy)_2Ru]_2BL_1^{4+}$ in 4:1 ethanol/ methanol excited at 436 nm: (a) the complex was purified by an ion-exchange column (dotted line); (b) the complex was purified by a silica gel column with 0.1 M NH_4PF_6 in MeOH as eluent (solid line).

The free BL_1 ligand shows two reduction waves at −0.77 and − 1.08 V (Figure 2). The difference between the reductions is about 0.3 V. Upon coordination to ruthenium, the complex shows four reduction waves at −0.29, −0.52, −1.45, and −1.68 V. Since the difference between the first two reductions is almost the same as that for the free ligand, we ascribe the reductions at −0.29 and −0.52 V as due to the reduction of the bridging ligand (eqs 5 and 6), whereas those at −1.45 and −1.68

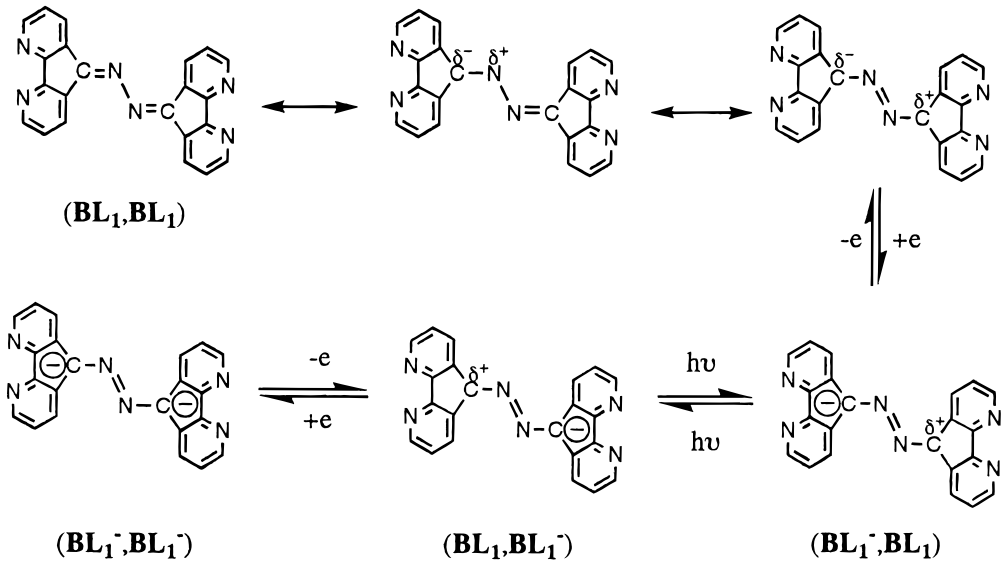

Figure 7. Resonance structures of BL_1 and its intervalence charge delocalization.

Table 4. Predicted UV−Visible Absorption Maxima Based on Electrochemistry Data

	$E_{1/2}$, V							
		1st redn						
complex	1st oxidn	BL	bpy	$\Delta E_{1/2}(1)$, V[a]	$\lambda_{1(max)}$, nm[b]	$\Delta E_{1/2}(2)$, V[c]	$\lambda_{2(max)}$, nm[d]	exptl λ_{max}, nm
$[(bpy)_2Ru]_2BL_1^{4+}$	1.38	−0.29	−1.45	1.67	743	2.83	438	444
$[(bpy)_2Ru]_2BL_2^{4+}$	1.32	−0.73	−1.24	2.05	605	2.56	485	442
$[(bpy)_2Ru]_2BL_3^{4+}$	1.37	−0.67	−1.27	2.04	608	2.64	470	444
$[(bpy)_2Ru]_2BL_4^{4+}$	1.32	−0.94	−1.56	2.26	549	2.88	431	441
$[(bpy)_2Ru(L_1)]^{2+}$	1.32	−0.86	−1.45	2.18	569	2.77	448	448
$[(bpy)_2Ru(L_2)]^{2+}$	1.36	−0.88	−1.46	2.24	554	2.82	440	441
$(bpy)_3Ru^{2+}$	1.28		−1.32			2.60	478	450

[a] $\Delta E_{1/2}(1) = E_{1/2}$(1st oxidn) − $E_{1/2}$(1st BL redn). [b] $\lambda_{1(max)}$ was calculated on the basis of $\Delta E_{1/2}(1)$ data. [c] $\Delta E_{1/2}(2) = E_{1/2}$(1st oxidn) − $E_{1/2}$(1st bpy redn). [d] $\lambda_{2(max)}$ was calculated on the basis of $\Delta E_{1/2}(2)$ data.

V correspond to reduction of each bipyridine ligand (eqs 7−10). The first ligand-based reductions of $[(bpy)_2Ru(BL_1)$-

$$[(b)(b)Ru^{II}(BL)Ru^{II}(b)(b)]^{4+} + e^- = [(b)(b)Ru^{II}(BL^-)Ru^{II}(b)(b)]^{3+} \quad (5)$$

$$[(b)(b)Ru^{II}(BL^-)Ru^{II}(b)(b)]^{3+} + e^- = [(b)(b)Ru^{II}(BL^{2-})Ru^{II}(b)(b)]^{2+} \quad (6)$$

$$[(b)(b)Ru^{II}(BL^{2-})Ru^{II}(b)(b)]^{2+} + e^- = [(b)(b^-)Ru^{II}(BL^{2-})Ru^{II}(b)(b)]^{+} \quad (7)$$

$$[(b)(b^-)Ru^{II}(BL^{2-})Ru^{II}(b)(b)]^{+} + e^- = [(b)(b^-)Ru^{II}(BL^{2-})Ru^{II}(b^-)(b)] \quad (8)$$

$$[(b)(b^-)Ru^{II}(BL^{2-})Ru^{II}(b^-)(b)] + e^- = [(b^-)(b^-)Ru^{II}(BL^{2-})Ru^{II}(b^-)(b)]^- \quad (9)$$

$$[(b^-)(b^-)Ru^{II}(BL^{2-})Ru^{II}(b^-)(b)]^- + e^- = [(b^-)(b^-)Ru^{II}(BL^{2-})Ru^{II}(b^-)(b^-)]^{2-} \quad (10)$$

$Ru(bpy)_2]^{4+}$ is shifted by 0.48 V from its value in the free ligand, indicating a great deal of stabilization of the bridging BL_1's π^* orbitals occurred upon coordination.[24]

The first reductions of the $[(bpy)_2RuL_1]^{2+}$, $[(bpy)_2RuL_2]^{2+}$, and $[(bpy)_2Ru(BL_4)Ru(bpy)_2]^{4+}$ complexes were irreversible, and hence their reductions are not comparable to the other three. In the case of the BL_2 and BL_3 dimers, the first reduction consisted of two closely spaced one-electron processes represently by eqs 5 and 6. Their second reduction may be associated with the second reduction of the bridging ligand rather than the bipyridine ligands as suggested by eqs 7−10. For the complexes $[(bpy)_2Ru(BL_1)Ru(bpy)_2]^{4+}$, $[(bpy)_2Ru(BL_2)Ru$-$(bpy)_2]^{4+}$, and $[(bpy)_2Ru(BL_3)Ru(bpy)_2]^{4+}$, the first reduction potential increases in the order $BL_1 < BL_3 < BL_2$. One might expect that as more phenyl spacers were added, the increased conjugation would give a systematic change. Apparently, resonance and ring rotation play important roles.

Resonance for the BL_1 ligand is illustrated in Figure 7. In this case charge delocalization is readily communicated across the molecule. For the BL_2 and BL_3 ligands, rotation about the phenyl ring apparently dampens this resonance effect and results in the observed anomaly for reduction of the bridging ligand.

Absorption Spectra. The absorption spectra of complexes having polyunsaturated bridging ligands represent a composite of intraligand ($\pi \rightarrow \pi^*$) and metal to bridging ligand charge transfer (MLCT). The lowest energy absorption in the complexes is MLCT and consists of overlapping $Ru(d\pi) \rightarrow BL$-(π^*) and $Ru(d\pi) \rightarrow bpy(\pi^*)$ transitions. The lowered symmetry removes the degeneracy of the π^* levels, which results in the appearance of broad MLCT bands. For mixed-ligand complexes, the interpretation becomes more complex, since there are multiple $d\pi \rightarrow \pi_1^*$ and $d\pi \rightarrow \pi_2^*$ transitions. However, as noted in Table 1, the absorption maxima of the first MLCT ($d\pi \rightarrow \pi_1^*$) bands are similar in energy for the various

(24) Arana, C. A.; Abruna, H. D. *Inorg. Chem.* **1993**, *32*, 194.

complexes, which means the d$\pi \rightarrow \pi_1$* (bpy) and d$\pi \rightarrow \pi_2$* (BL,L) transitions cannot be separated from one another as observed for other analogous series.[25,26] In contrast to the case of $Ru(bpy)_3^{2+}$, the absorption maxima are blue-shifted for all the dimer complexes, but they are red-shifted compared to the case of $Ru(bpy)_2(dafo)^{2+}$.

It is now well established that the lowest energy MLCT transitions (λ_{max}) are, for a related class of ligands, linearly related to the difference between the potential for the first one-electron reduction (LUMO) and the first one-electron oxidation (HOMO) ($\Delta E_{1/2}$).[27] In all of the complexes reported here, the oxidation is localized on the ruthenium center and the first reduction is localized on the bridging ligand. Electrochemical data were used to calculate the expected energy transitions for the MLCT bands and are listed in Table 4. As a result, the lowest energy MLCT transition is expected to be Ru(dπ) $\rightarrow$ BL(π*) and occur in the near-IR region of the spectrum, but experimentally no absorptions in this region were observed. The MLCT bands more closely match the Ru(dπ) $\rightarrow$ bpy(π*) transitions, e.g. 450 nm for $Ru(bpy)_3^{2+}$, which suggests the Ru(dπ) $\rightarrow$ BL(π*) transitions are somehow forbidden. The reason for this is not known at present, but it is consistent with the lack of the normally observed red shift in the absorption maxima (MLCT) among the dimer complexes.[1a,28]

The magnitude of the absorption coefficients for the d$\pi \rightarrow \pi$* transitions are related to the number of diimine ligands as reported earlier.[29] On the basis of observations of Rillema and co-workers,[30] the absorption coefficients for the bimetallic complexes are expected to be larger than those for the monomers. As noted from redox potentials, the thermodynamic characteristics of the dimer complexes indicate that the metal centers are noninteracting in the ground state, since the $Ru^{III/II}$ redox processes of both metal centers occur at, or near, the same potenial. Therefore absorption coefficients for the MLCT transitions of these complexes should be approximately twice as large as those for the analogous monomers. The data shown in Table 1 are consistent with this.

Photophysical Behavior. Emission properties of polypyridyl ruthenium(II) complexes generally follow the energy gap law.[29] The ^{3}MLCT state is reasonably long-lived and is thought to be deactivated by three processes: radiative decay, k_r, radiationless decay, k_{nr}, and thermal population of a higher lying excited state, $k_1 \exp(-\Delta E/RT)$. For the last process, the thermally accessible excited state has been designated as a ligand field (LF) excited state. The energy of this presumed LF state should depend on the ligand field strength. Emission intensity and temperature-dependent emission lifetimes follow the model shown in Figure 8 originally proposed by Crosby et al.,[31] Meyer,[32] and others.[33]

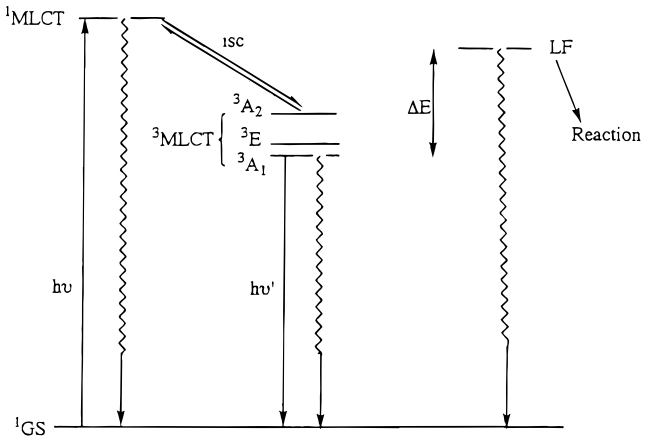

Figure 8. Energy state diagram based on the Crosby−Meyer model.

Van Houten and Watts were able to evaluate the energy difference between these two states (ΔE) as 3600 cm^{-1} in water for ruthenium tris(bipyridine).[34] The values of ΔE (Table 3) for the dimer complexes are substantially lower than the corresponding value for $Ru(bpy)_3^{2+}$. These results are consistent with ligand field theory, since diazafluorenone derivatives are known to be lower than bipyridine in the spectrochemical series.[9] Therefore, the LF excited-state energy will be lowered if bipyridine ligands are replaced by diazafluorenone derivatives. Consequently, population of the LF state is very efficient for these complexes at room temperature and these complexes are essentially nonemissive at room temperature, an observation which is consistent with the report of Cherry et al.[35] Emission lifetimes at room temperature were obtained from extrapolation based on temperature-dependent lifetime measurements as shown in Table 3 and are inversely related to the distances of the two ruthenium ions of the dimer complexes: $[(bpy)_2Ru]_2BL_1^{4+}$ (12.4 Å, 0.36 ns) > $[(bpy)_2Ru]_2BL_2^{4+}$ (14.9 Å, 0.12 ns) > $[(bpy)_2Ru]_2BL_3^{4+}$ (19.2 Å, 0.10 ns).

Finally, there is a parallel between the observed absorption and emission maxima. The difference between the first electrochemical oxidation and reduction would place the emission maximum in the near-infrared region of the spectrum. Since the Ru(dπ) $\rightarrow$ BL(π*) transitions appear to be forbidden, the observed luminescence spectra are most likely ascribable to transitions involving the terminal bipyridine ligands, not the BL ligand.

Acknowledgment. We thank the Office of Basic Energy Sciences of the Department of Energy for support, the National Science Foundation for the laser equipment, and Johnson Matthey for the loan of the source ruthenium compound.

IC970534+

(25) (a) Rillema, D. P.; Taghdiri, D. G.; Jones, D. S.; Keller, C. D.; Worl, L. A.; Meyer, T. J.; Levy, H. A. *Inorg. Chem.* **1987**, *26*, 578. (b) Rillema, D. P.; Mack, K. B. *Inorg. Chem.* **1982**, *21*, 3849. (c) Rillema, D. P.; Callahan, R. W.; Mack, K. B. *Inorg. Chem.* **1982**, *21*, 2589.
(26) Durham, B.; Casper, J. K.; Nagle, J. K.; Meyer, T. J. *J. Am. Chem. Soc.* **1982**, *104*, 4803.
(27) Boyde, S.; Strouse, G. F.; Jones, W. E., Jr.; Meyer, T. J. *J. Am. Chem. Soc.* **1990**, *112*, 7395.
(28) Elliott, C. M.; Hershenhart, E. J. *J. Am. Chem. Soc.* **1982**, *104*, 7519.
(29) (a) Sahai, R.; Baucom, D. A.; Rillema, D. P. *Inorg. Chem.* **1986**, *25*, 3843. (b) Van Wallendael, S.; Shaver, R. J.; Rillema, D. P.; Yoblinski, B. J.; Stathis, M.; Guarr, T. *Inorg. Chem.* **1990**, *29*, 167. (c) Van Wallendael, S.; Perkovic, M. W.; Rillema, D. P. *Inorg. Chim. Acta* **1993**, *213*, 253.
(30) Macatangay, A.; Zheng, G. Y.; Rillema, D. P.; Jackman, D. C.; Merkert, J. W. *Inorg. Chem.* **1996**, *35*, 6823.
(31) (a) Hager, G. D.; Crosby, G. A. *J. Am. Chem. Soc.* **1975**, *97*, 7031. (b) Hager, G. D.; Watts, R. J.; Crosby, G. A. *J. Am. Chem. Soc.* **1975**, *97*, 7037. (c) Hipps, K. W.; Crosby, G. A. *J. Am. Chem. Soc.* **1975**, *97*, 7042.
(32) (a) Meyer, T. J. *Pure Appl. Chem.* **1990**, *62*, 1003. (b) Meyer, T. J. *Pure Appl. Chem.* **1986**, *58*, 1193.
(33) (a) Barigelletti, F.; Belser, P.; von Zelewsky, A.; Juris, A.; Balzani, V. *J. Phys. Chem.* **1985**, *89*, 3680. (b) Barigelletti, F.; Belser, P.; von Zelewsky, A.; Juris, A.; Balzani, V. *J. Phys. Chem.* **1986**, *90*, 5190. (c) Watts, R. J. *J. Chem. Educ.* **1983**, *60*, 834 and references therein.
(34) Van Houten, J.; Watts, R. J. *J. Am. Chem. Soc.* **1976**, *98*, 4853.
(35) Wacholtz, W. M.; Auerbach, R. A.; Schmehl, R. H.; Ollino, M.; Cherry, W. R. *Inorg. Chem.* **1985**, *24*, 1758.